SCHOOL OF MATERIALS AND MINERAL RESOURCES ENGINEERING
UNIVERSITI SAINS MALAYSIA

INVESTIGATION OF Ni/Cu AS OHMIC CONTACT ON P-TYPE GaN

By

KOE MEI YEN

SUPERVISOR: PROFESSOR DR. IR. CHEONG KUAN YEW

Dissertation submitted in partial fulfillment
of the requirements for the degree of Bachelor of Engineering with Honours
(Materials Engineering)

Universiti Sains Malaysia

JUNE 2017

DECLARATION

I hereby declare that I have conducted, completed the research work and written the dissertation entitles **"Investigation of Ni/Cu as Ohmic contact on p-type GaN"**. I also declared that it has not been previously submitted for the award for any degree or diploma or other similar title of this for any other examining body or University.

Name of Student : Koe Mei Yen Signature:

Date : 22 JUNE 2017

Witnessed by

Supervisor : Prof. Ir. Dr. Cheong Kuan Yew Signature:

Date : 22 JUNE 2017

ACKNOWLEDGEMENTS

First and foremost, I would like to express my deepest appreciation to Universiti Sains Malaysia, especially School of Materials and Mineral Resources Engineering for providing an appropriate and healthy environment as well as resources and necessary infrastructure to accomplish my final year project of Bachelor's Degree in Materials Engineering.

On top of that, I would like to express my utmost gratitude to my helpful and respectful supervisor, Prof. Ir. Dr. Cheong Kuan Yew for the support, guidance, sharing and encouragements throughout the semester to complete my research project. Besides, the expertise comments, constructive suggestion, regularly followed up on my progress and went through my work despite his busy schedule have provided a high quality basis for the present thesis.

Furthermore, I am immensely grateful to all laboratory, academic and administrative staffs for the great help in utilization of equipment and recommendations in solving problem throughout the project. I am also grateful to my beloved course mates and friends for continuous helping and support during my year of academic achievements.

Last but not least, I also place on record, my sense of gratitude to all who directly or indirectly have lent their hand in completing this work.

TABLE OF CONTENTS

Contents	**Page**
DECLARATION	ii
ACKNOWLEDGEMENTS	iii
TABLE OF CONTENTS	iv
LIST OF TABLES	vii
LIST OF FIGURES	viii
LIST OF ABBREVIATIONS	xi
LIST OF SYMBOLS AND UNITS	xiv
ABSTRAK	xvi
ABSTRACT	xviii
CHAPTER 1 INTRODUCTION	1
1.1 Research Background	1
1.2 Problem Statement	4
1.3 Research Objectives	5
1.4 Project Overview	6
CHAPTER 2 LITERATURE REVIEW	7
2.1 Gallium Nitride	7
2.2 Motivation for p-GaN Ohmic Contact Work	9

2.3 Metal System with their Low Specific Contact Resistivity 10

2.4 Cu-Ni Alloys 16

2.4.1 General Information on Cu-Ni Alloys 16

2.4.2 The Cu-Ni equilibrium diagram 16

2.5 Circular Transmission Line Model (CTLM) 18

2.5.1 Basic Concept of CTLM 18

2.5.2 Derivation of Specific Contact Resistance 19

2.6 Physics of metal-semiconductor contact 23

2.6.1Schottky-Mott Model 23

2.6.2 Barden Model 27

CHAPTER 3 MATERIALS AND METHODOLOGY 29

3.1 Overview 29

3.2 Experimental procedures 29

3.3 Fabrication procedures 30

3.4 Photolithography Process 37

3.4.1 Emulsion Mask Design and Preparation 37

3.4.2 Fabrication of Emulsion Mask 37

3.4.3 Spin Coating of Photoresist 39

3.4.4 Deposition of Pattern on GaN Substrate 39

3.4.5 Electrical Charactirization 40

3.5 Experiment Parameters 42

3.6 Characterization Techniques 43

3.6.1 Characterization by Atomic Force Microscope (AFM) 43

3.6.2 Characterization by X-ray Diffraction (XRD) 45

3.6.3 Characterization by Field Emission Scanning Electron Microscopy (FESEM) Equipped with Energy Dispersive X-ray (EDX) 47

CHAPTER 4 RESULTS AND DISCUSSION 50

4.1 AFM analysis 50

4.2 XRD analysis 56

4.3 Electrical Characterization 64

4.3.1 Variation of specific contact resistance, ρ_c with respect to Ni/Cu composition 64

4.3.2 Variation of specific contact resistance, ρ_c with respect to annealing temperature 71

4.4 FESEM and EDX analysis 79

CHAPTER 5 CONCLUSION AND RECOMMENDATIONS 82

5.1 Conclusion 82

5.2 Recommendations 83

REFERENCES 84

APPENDICES 89

LIST OF TABLES

		Page
Table 2.1:	Metal contacts with the lowest specific contact resistances (ρ_c), the thickness of metal layers, doping concentration of GaN and annealing conditions are indicated. Contacts are arranged in ascending order of ρ_c.	12
Table 2.2:	Summary of the behavior of contacts on p-type semiconductors under the 2 workfunction conditions: $q\varphi_m > q\varphi_s$ and $q\varphi_m < q\varphi_s$.	25
Table 3.1:	Parameters altered in the experiment.	42
Table 4.1:	Results of AFM analysis by Nanonavi software for GaN substrate annealing at 550°C, 600°C, 650°C, 700°C.	51
Table 4.2:	Specific contact resistance for GaN substrate deposited with different composition of Ni/Cu annealed at various temperature when supply with reverse voltage, 0 V to -2 V.	69
Table 4.3:	Specific contact resistance for GaN substrate deposited with different composition of Ni/Cu annealed at various temperature when supply with forward voltage, 0 V to 2 V.	70

LIST OF FIGURES

		Page
Figure 2.1:	Cu-Ni equilibrium diagram.	17
Figure 2.2:	Test pattern for Ohmic contact characterization: Circular pattern, where r_o is the radii of the inner circular contact; r_i is the radii of the outer region; and d is the difference between r_o and r_i.	18
Figure 2.3:	Experimental setup for deviation of specific contact resistance.	19
Figure 2.4:	Graph of R_T versus d used to calculate specific contact resistance ρ_c of metal contact.	21
Figure 2.5:	Energy band diagrams of metal-semiconductor contacts	24
Figure 2.6:	P-type metal-semiconductor contacts with surface states	28
Figure 3.1:	Schematic diagram of the layer structure of Mg-doped p-GaN on sapphire substrate.	30
Figure 3.2:	Flow chart of fabrication and characterization of Ni/Cu contacts to p-GaN.	31
Figure 3.3:	Fundamental process of fabricating the GaN substrate.	32
Figure 3.4:	GaN substrate cut into dimension of 1 cm x 1 cm.	33
Figure 3.5:	Layout of (a) an individual circular-TLM structure, (b) circular-TLM structures used for measurements.	34
Figure 3.6:	Dimensions of CTLM formed observed under OM (a) gap (b) inner diameter	36
Figure 3.7:	Master mask film	38
Figure 3.8:	Emulsion mask	38
Figure 3.9:	Placement of probe on sample.	41
Figure 3.10:	(a) A new AFM tip; inset: The end of the new tip, (b) A used AFM tip.	44
Figure 3.11:	AFM is working with an optical lever.	45

Figure 3.12:	Basic features of a typical XRD.	46
Figure 3.13:	Schematic drawing illustrates the signals generated inside a scanning electron microscope when an electron beam interacts with a specimen.	49
Figure 3.14:	Samples that mounted.	49
Figure 4.1:	Surface roughness of GaN substrate with different composition of Ni/Cu at annealing temperature (a) 550°C, (b) 600°C, (c) 650°C, (d) 700°C.	52
Figure 4.2:	Surface roughness of GaN substrate annealed at various temperature with composition (a) Ni/Cu (60 s/60 s), (b) Ni/Cu (45 s/15 s), (c) Ni/Cu (30 s/30 s), (d) Ni/Cu (15 s/45 s).	55
Figure 4.3:	XRD pattern of Ni/Cu (60 s/60 s) deposited on GaN at (a) different annealing temperature, (b) annealing temperature 600°C.	57
Figure 4.4:	XRD pattern of Ni/Cu (45 s/15 s) deposited on GaN at (a) different annealing temperature, (b) annealing temperature 700°C.	59
Figure 4.5:	XRD pattern of Ni/Cu (30 s/30 s) deposited on GaN at different annealing temperature.	61
Figure 4.6:	XRD pattern of Ni/Cu (15 s/45 s) deposited on GaN at (a) different annealing temperature, (b) annealing temperature 550°C.	63
Figure 4.7:	Plot of measured total resistance (R_T) against the gap spacing for different composition of Ni/Cu annealed at 550°C with (a) reverse voltage supply, 0 V to -2 V, (b) forward voltage supply, 0 V to 2 V	65
Figure 4.8:	Plot of measured total resistance (R_T) against the gap spacing for different composition of Ni/Cu annealed at 600°C with (a) reverse voltage supply, 0 V to -2 V, (b) forward voltage supply, 0 V to 2 V	66
Figure 4.9:	Plot of measured total resistance (R_T) against the gap spacing for different composition of Ni/Cu annealed at 650°C with (a) reverse voltage supply, 0 V to -2 V, (b) forward voltage supply, 0 V to 2 V	66

Figure 4.10: Plot of measured total resistance (R_T) against the gap spacing for different composition of Ni/Cu annealed at 700°C with (a) reverse voltage supply, 0 V to -2 V, (b) forward voltage supply, 0 V to 2 V 67

Figure 4.11: Plot of measured total resistance (R_T) against the gap spacing for Ni/Cu (60 s/60 s) annealed at various temperature with (a) reverse voltage supply, 0 V to -2 V, (b) forward voltage supply, 0 V to 2 V 71

Figure 4.12: Plot of measured total resistance (R_T) against the gap spacing for Ni/Cu (45 s/15 s) annealed at various temperature with (a) reverse voltage supply, 0 V to -2 V, (b) forward voltage supply, 0 V to 2 V 72

Figure 4.13: Plot of measured total resistance (R_T) against the gap spacing for Ni/Cu (30 s/30 s) annealed at various temperature with (a) reverse voltage supply, 0 V to -2 V, (b) forward voltage supply, 0 V to 2 V 72

Figure 4.14: Plot of measured total resistance (R_T) against the gap spacing for Ni/Cu (15 s/45 s) annealed at various temperature with (a) reverse voltage supply, 0 V to -2 V, (b) forward voltage supply, 0 V to 2 V 73

Figure 4.15: Specific contact resistance of GaN substrate annealed at various temperature with different composition of Ni/Cu with reverse voltage supply, 0 V to -2 V 75

Figure 4.16: Specific contact resistance of GaN substrate annealed at various temperature with different composition of Ni/Cu with forward voltage supply, 0 V to 2 V 77

Figure 4.17: (a) FESEM micrograph and (b) EDX spectra of GaN deposited with Ni/Cu (60 s/60 s) annealed at 650°C 80

Figure 4.18: (a) FESEM micrograph and (b) EDX spectra of GaN deposited with Ni/Cu (60 s/60 s) annealed at 550°C 81

LIST OF ABBREVATIONS

SiC	Silicon carbide
GaN	Gallium Nitride
UV	Ultraviolet
HEMT	High Electron Mobility Transistors
Si	Silicon
Au	Gold
Ti	Titanium
AlGaN	Aluminium Gallium Nitride
Al	Aluminium
Ni	Nickel
Cu	Copper
Mg	Magnesium
p-GaN	Positively doped GaN
CTLM	Circular Transmission Line Model
MESFET	Metal-Semiconductor Field-Effect Transistor
HBT	Heterojunction Bipolar Transistor
RCA	Radio Corporation of America
H_2O_2	Hydrogen Peroxide
NH_4OH	Ammonium Hydroxide
HF	Hydrogen Fluoride
AFM	Atomic Force Microscopy
SPA	Semiconductor Parameter Analyzer
BSE	Back-Scattered Electron

DC	Direct Current
EDX	Energy Dispersive X-Ray Spectroscopy
FESEM	Field Emission Scanning Electron microscopy
ICCD	International Centre for Diffraction Data
MOCVD	Metal-Organic Chemical Vapour Deposition
RMS	Root Mean Square
Ra	Average roughness
IPA	Isopropyl Alcohol
GaNi	Gallium Nickel
XRD	X-Ray Diffraction
$CuGaO_2$	Copper(i) Gallium Oxide
OM	Optical Microscope
N_2NiO_6	Nickel Bis
e-	Electron
ECB	Conduction band energy
EDX	Energy dispersive X-ray
EVB	Valence band energy
FESEM	Field emission scanning electron microscope
h+	Hole
UV	Ultra-violet
O / O_2	Oxygen
NiO	Nickel Oxide
H_2O	Water
DI	Dionised Water
ρ_c	Specific Contact Resistance

R_T	Total Resistance
CuO	Copper Oxide
N / N_2	Nitrogen
LED	Light Emitting Diode
I-V	Current-Voltage
HNO_3	Nitric Acid
HF	Hydroflouric Acid

LIST OF SYMBOLS AND UNITS

%	Percentage
°	Degree
°C	Degree Celcius
Å	Angstrom
cm	Centimeter
Eg	Optical Energy Band Gap
eV	Electron Volt
mbar	millibar
rpm	Rotation per minute
min	Minute/s
mm	millimeter
N_d	Number of Dopant
nm	Nanometer
Pa	Pascal
Ra	Surface Roughness
W	Watt
z	Atomic Number
θ	Theta
λ	wavelength
μm	Micrometer
d_{hk}	Interplanar spacing in crystal
θ_{hkl}	Angle between diffracted and transmitted beams

Ω	Ohm
Ωcm^2	Ohm per centimeter square
R_T	Total resistance
r_i , r_o	Inner and Outer radii of circular contact
I_o, I_1, K_o, K_1	Modified Bessel Functions
L_T	Transfer length
R_s	Semiconductor sheet resistance
d	Distance between inner and outer contact pads
i	Current across separation d
E_F	Fermi energy
$q\chi$	Electron affinity of semiconductor
E_g	Bandgap energy of semiconductor
$q\varphi_{Bp}$	Schottky barrier height of p-type semiconductor
$q\varphi_m$	Workfunction of Metal
$q\varphi_s$	Workfunction of Semiconductor
$q\varphi_o$	Neutral Energy Level

PENYELIDIKAN KENALAN OHMIC NI/Cu DI ATAS GaN JENIS POSITIVE

ABSTRAK

Pada masa kini, semikonduktor jurang jalur lebar seperti Gallium Nitrida (GaN) dianggap sebagai bahan yang paling menjanjikan untuk peranti elektronik kuasa generasi akan datang. Ciri-ciri GaN seperti jurang band lebar, medan elektrik kritikal yang tinggi dan kekonduksian terma yang tinggi memberi kemungkinan untuk mengarang peranti yang beroperasi pada voltan, suhu dan frekuensi yang lebih tinggi berbanding dengan Silikon. Peranti berdasarkan bahan jurang jalur lebar membolehkan pengurangan kuasa yang ketara dan peningkatan kecekapan tenaga. Dalam projek ini bertujuan untuk mengkaji kesan komposisi dan kombinasi Ni / Cu yang berbeza pada hubungan Ohmic antara logam dan p-GaN, kesan suhu penyepuhlahan yang berbeza pada hubungan Ohmic antara logam dan p-GaN dan untuk menyiasat hubungan tertentu. Rintangan tertentu di antara logam dan semikonduktor melalui model garis pekeliling Circular (CTLM) diselidik dengan mengubah radius dalaman dan jurang. Corak dihasilkan menggunakan proses photolithography. Tembaga (Cu) dan nikel (Ni) didepositkan menggunakan kaedah penyejatan haba. Ni telah didepositkan dahulu, diikuti oleh Cu pada Templat M-doped P-GaN (0001) pada Sapphire. Ketebalan logam yang disimpan dikawal dengan memanipulasi masa pemendapan dalam lingkungan 15 s hingga 60 s. Suhu penyepuhlindapan 550 ° C, 600 ° C, 650 ° C dan 700 ° C digunakan untuk setiap komposisi. AFM digunakan untuk menentukan morfologi permukaan sampel. XRD digunakan untuk mengenal pasti fasa yang ada di dalam sampel dan FESEM digunakan untuk menentukan ketebalan logam yang disimpan dan EDX digunakan untuk mengenal pasti elemen pada sampel. Pencirian elektrik telah diperolehi menggunakan mesin SPA dan rintangan hubungan tertentu kenalan Ohmic boleh ditentukan. Apabila voltan terbalik

0 v hingga -2 V dan voltan ke hadapan 0 v hingga 2 V dibekalkan, sampel dengan rintangan hubungan spesifik terendah, ρc 8.399 x 1011 Ωcm^2 dan 7.299 x 1012 Ωcm^2 masing-masing adalah Ni / Cu (150 nm / 150 nm) menyepuhlindap pada 550 ° C. Kekasaran permukaan Ra dan RMS masing-masing adalah 64.63 nm dan 86.35 nm yang menyiasat menggunakan AFM. Dari hasil XRD, fasa yang hadir untuk sampel ini ialah CuO (110), CuO $(11\bar{1})$ dan GaN (222).

INVESTIGATION OF Ni/Cu AS OHMIC CONTACT ON P-TYPE GaN

ABSTRACT

Nowadays, wide band gap semiconductors like Gallium Nitride (GaN) are considered the most promising materials for the next generation of power electronic devices. The properties of GaN like wide band gap, high critical electric field and high thermal conductivity give the possibility to fabricate devices operating at much higher voltages, temperatures and frequencies than in Silicon. Devices based on wide band gap materials enable a significant reduction of the power losses and an increase of the energy efficiency. In this project aims to study the effect of different composition and combination of Ni/Cu on the Ohmic contact between metal and p-GaN, the effect of different annealing temperature on the Ohmic contact between metal and p-GaN and to investigate the specific contact resistivity at the interface between the metal and the semiconductor through Circular transmission line model (CTLM) via varying the inner radius and gap. The pattern were produced using photolithography process. Copper (Cu) and nickel (Ni) were deposited using thermal evaporation method. Ni were deposited first, followed by Cu on the Mg-doped P-type GaN (0001) on Sapphire. The thickness of metal deposited were controlled by manipulating the deposition time in the range of 15 s to 60 s. The annealing temperature 550°C, 600°C, 650°C and 700°C were applied to each of the composition. AFM were used to determine the surface morphology of the sample. XRD were used to identify the phase present in the sample. Electrical characterization were obtained using SPA machine and specific contact resistance of the Ohmic contact can be determined. When reverse voltage 0 v to -2 V and forward voltage 0 v to 2 V supplied, the sample with lowest specific contact resistance, ρ_c 8.399 x 10^{11} Ωcm^2 and 7.299 x 10^{12} Ωcm^2 respectively is Ni/Cu (150 nm/150 nm) annealed at 550°C. The surface

roughness Ra and RMS are 64.63 nm and 86.35 nm respectively which investigate using AFM. From XRD result, the phase present for this sample are CuO (110), CuO ($11\bar{1}$) and GaN (222). From FESEM, the thickness of metal obtained for this sample were about 300 nm and EDX were used to identify the element on the sample.

CHAPTER 1

INTRODUCTION

1.1 Research Background

In this day and age, wide band gap semiconductors, such as silicon carbide (SiC) and gallium nitride (GaN), are considered as promising materials for the future generation of high power and radio frequency applications. GaN-based heterostructures have been found suitable for its application in electronics and optoelectronics devices operating in the blue and ultraviolet (UV) region of the light spectrum. This is due to their extraordinary physical properties, like a high critical electric field (2–4 MV/cm), wide band gap (>3 eV), and low intrinsic carrier concentration (10^{-9}–10^{-10} cm^{-3}). This allow the possibility to fabricate devices that can operate at much higher temperatures, voltages, and frequencies compared to silicon. In addition to that, devices based on wide band gap materials enable a significant increase of the energy efficiency and reduction of the power losses (Upadhyay et al., 2015).

SiC showed a considerable maturity with respect to the device performances and present material quality. While, GaN materials and devices still suffer from the limited performances and reliability issues. To grow AlGaN/GaN heterostructures, two dimensional electron gas need to be generated at the interface by the piezoelectric polarization gradient. Due to the presence of two dimensional electron gas, high electron mobility transistors (HEMTs) based on GaN can produce a low channel resistance with respect to Si and SiC devices. Since Ohmic contacts act as the link between the device and the external circuit, Ohmic contacts are the fundamental building blocks of power devices. In order to minimize

the device specific contact resistance (ρ_c), their resistance must be negligible with respect to the semiconductor drift layer and the power losses of the system. Low resistance Ohmic contact is an integral part for any device and a lot of efforts are being directed to improve the characteristics of the Ohmic contacts to GaN and related heterostructures. Efforts are being directed to improve the surface condition for Ohmic contact formation by pre-processing techniques electronic devices based on wide band gap semiconductors require specific contact resistance (ρ_c) values in the typical range of 10^{-5}–10^{-6} Ωcm^2 (Greco et al., 2016).

An ideal Ohmic contact is defined as, no barriers to the carrier flow are encountered in either positive or negative direction when combined with semiconductor. This condition will occur ideally when works functions of the semiconductor and metal are about the same, and there are no appreciable interface states which tend to the pinning of Fermi Level. In order to realize the potential of GaN devices, a good metallization, especially for Ohmic contact, is essential. The Ohmic contact must fulfill the requirements of low contact resistance, smooth surface morphology, and good edge acuity (Wong et al., 2013).

The most commonly used Ohmic contact for AlGaN/GaN HEMT devices is alloy of a multilayer metal structure that consists of Ti/Al metal layers. A low resistance alloy can be formed upon annealing at high temperature (750–950°C). Ti/Al is prone to oxidation, so an oxidation prevention layer such as gold (Au) is deposited on Ti/Al to protect the Ohmic contact for long term device operation. In addition to that, a barrier layer (such as Ni, Pt, Cr, or Mo) is also needed to prevent Au from diffusing into GaN during thermal annealing process. By optimizing the Ohmic contact formation parameters, specific contact resistances

(ρ_c) as low as 7.3 x 10^{-7} Ωcm^2 (Wenzel et al., 2001) and 4.7 x 10^{-7} Ωcm^2 (Guo et al., 1996) have been demonstrated using Ti/Al/Ni/Au and Ti/Al/Mo/Au Ohmic structure, respectively.

Nevertheless, the gold cost is increasing from time to time and on a long-term basis the search for an alternative material to replace the Au layer for GaN device metallization is required. The metal copper (Cu) is a potential candidate because Cu is lower in cost, lower resistivity and higher thermal conductivity as compared to Au. Therefore, the Cu has been widely used for multi-level interconnects in the silicon VLSI technology (Schmitz et al., 1998, Adivarahan et al., 2001).

These advantages will increase the use of Cu metallization on GaN devices. Recently, Cu has been demonstrated to perform well as gate contacts (Shen et al., 1992) and as interconnects (Nakamura et al., 1993) on the GaN HEMTs. Nevertheless, the diffusion of Cu into GaN at elevated temperatures can be detrimental to the GaN devices and affect the device performance (Chen et al., 1999)

An effective diffusion barrier to Cu is thus required, especially for the Ohmic contact. A few Ohmic contact structures for GaN devices, such as Si/Ti/Al/Cu/Au (Koide et al., 1999) and Ge/Cu/Ge (Waki et al., 2000) have been investigated. Although Ohmic contacts could be achieved at relatively lower temperatures (<800°C) for these structures, they all suffer from having high contact resistance ($\rho_c > 10^{-5}$ Ωcm^2). The role of Ni as an adhesion and diffusion barrier layer is examined. The study showed that, with an optimized Ni layer thickness, a low contact resistance and smooth surface morphology can be achieved with the Ti/Al/Ni/Cu Ohmic contact (Waki et al., 2000).

1.2 Problem Statement

Regards of these recent successes in the development of GaN-based devices, the fabrication of Ohmic contacts with low specific contact resistance (ρ_c) is a great technological that is importance to the industry. However, the high ρ_c of the p-type Ohmic contact is one of the major problems faced in the realization of long-lifetime operation of GaN-based optical devices. It indicated the high ρ_c of p-GaN limits the efficiency of GaN-based devices.

However, there are some physical difficulties in the formation of good Ohmic contacts to p-type GaN. First, it is difficult to obtain a low metal/p-GaN barrier height because the wide band gap of the material (3.4 eV), and the typical values of the metal work functions is about the range of 4–5 eV. In addition to that, another important issue is related to the difficulty to grow a heavily-doped p-GaN (>10^{18} cm^{-3}) with high free holes concentration. Magnesium (Mg) is the most efficient p-type dopant species for GaN.

Despite the fact of significant progresses on the p-type doping techniques and electrical activation have been reported by Amano and Nakamura (Akasaki et al., 2014), the Mg-acceptors with the high ionization energy which about the range 150–200 meV, depends on the active acceptor concentration, and the free holes concentration in p-type GaN were strongly limits at room temperature. In addition to that, the formation of Mg-H complexes will further reduces the free holes concentration. So a high Mg concentration (>$10^{19}cm^{-3}$) can be incorporated during p-GaN growth. The free holes concentration in the range 10^{17}–10^{18} cm^{-3} can be achieved in the material. To improve the above issues, the use of alloyed metal compounds and specific annealing conditions are implemented to increase the active

carrier concentration below the interface and reduce the effective metal/p-GaN barrier height (Greco et al., 2016).

The ever rising gold cost on a long term basis has fueled the search for an alternative material to replace the Au layer for GaN device metallization. Cu as a potential candidate with the properties like lower resistivity and higher thermal conductivity as compared to Au is worth to study.

1.3 Research Objectives

The objectives of this research are as follow:

- To determine the effect of different composition of Ni/Cu on the Ohmic contact between metal and p-GaN.
- To study the effect of different annealing temperature on the Ohmic contact between metal and p-GaN.
- To investigate the specific contact resistivity at the interface between the metal and the semiconductor through Circular Transmission Line Model (CTLM) via varying the inner radius and gap.

1.4 Project Overview

In this project, different thickness of metal (Ni/Cu) were deposited using thermal evaporation method and annealed at different temperature (550°C, 600°C, 650°C, 700°C). The effect of the composition and annealing temperature towards the surface morphology, the compositional change and the specific contact resistance were studied. The CTLM structure with different inner diameter and various gap is implemented to investigate the effect on the specific contact resistivity.

CHAPTER 2

LITERATURE REVIEW

2.1 Gallium Nitride

Research on the properties of Gallium Nitride (GaN) has increased drastically starting the announcement of the development of blue Light Emitting Diodes (LEDs) using GaN . There are various reports that have shown the successful usage of GaN in metal-semiconductor field-effect transistors (MESFETs) (Asif Khan et al., 1993), UV photoconductive detectors (Khan et al., 1992), heterojunction bipolar transistors (HBTs) (Pankove et al., 1994), high electron mobility transistors (HEMTs) (Asif Khan et al., 1993) and laser diodes (LDs) (Nakamura et al., 1996). This is due to GaN being a wide energy bandgap material (~3.4 eV at 300K) compared to GaAs (1.42 eV) and Si (1.12 eV). The wide band gap of GaN allows it for high-temperature operations, since it has the lower possibility for valence electrons to spontaneously jumping into the conduction band during these operations. Wide-bandgap semiconductors also generate less noise, hence GaN is a suitable material for making of highly sensitive detectors in the UV range (Khan et al., 1992). In addition, GaN has a high thermal conductivity of 130 W/mK, which is comparable to the thermal conductivity of Si (149 W/mK). In addition to those properties, GaN is being found to be chemically stable at high temperatures; making it excellent for highly efficient optoelectronic devices, like those mentioned earlier (Ueda, 2017).

Initially, conducting p-type GaN was too elusive to launch a massive effort on devices like LEDs. Continuous work on p-type GaN by Drs. Akasaki, Amano, Van Vechten and Nakamura has made possible the fabrication of high brightness visible LEDs especially in the blue part of the spectrum. It is a great challenge to produce low-resistance Ohmic contacts to p-GaN. The major problem impeding low-resistance Ohmic contacts on p-GaN is the small carrier density of the Mg-doped p-GaN. The Mg doping concentration is generally about 10^{20} cm^{-3}, but only 0.1–1% of the Mg atoms are activated, due to high activation energy (170 meV) and the formation of Mg–H complexes decreasing the number of active carriers which leads to carrier densities approximately 5 x 10^{17} cm^{-3}. The low free carrier concentration in the p-type layer limits the tunneling current typically responsible for low-resistance contacts. Secondly, a high barrier height (7 eV) would be expected for metals on p-GaN due to the large band gap (3.4 eV) and the electron affinity close to 4.1 eV for GaN. Studies on p-GaN contacts are still in progress to achieve a better specific contact resistivity. Favorable values for a low contact resistance are below 10^{-4} Ωcm^2 (Akasaki et al., 2014).

The resistance of an Ohmic contact on a specific semiconductor is determined by four major factors: (i) the fabrication of semiconductor itself (the GaN epilayer), (ii) the preparation technique of the contact structure prior to contact deposition mainly refer to the treatment of the semiconductor surface, (iii) the choice of the contact materials and their deposition, (iv) the treatment of this contact by thermal annealing (Chuah et al., 2010).

2.2 Motivation for p-GaN Ohmic Contact Works

An ideal Ohmic contact with no barriers to the carrier flow are encountered in either positive or negative direction when metal combined with semiconductor. Ideally, this occurs when work functions of the semiconductor and metal are about the same, and there are no appreciable interface states which tend to the pinning of Fermi Level. However, it is not possible as the work function of the semiconductor varies with doping concentration and for wide bandgap semiconductor such as p-GaN, there is an added difficulty because it is impossible to find a metal that has a large enough work function. Hence, it is not an easy task to achieve a good Ohmic contact between p-GaN and metal (Lim woon chi, 2006). Due to their high energy bandgap and high electron saturated velocity, the AlGaN/GaN high electron mobility transistor (HEMT) has become an ideal device for high frequency and high power applications. In order to realize the potential of GaN devices, a good metallization, especially for Ohmic contact, is essential. The Ohmic contact must fulfill the requirements of low contact resistance, smooth surface morphology, and good edge acuity (Wong et al., 2013).

However, the high ρ_c p-type Ohmic contact poses one of the major problems in the realization of long-lifetime operation of GaN-based optical devices. In short, the high ρ_c of p-GaN limits the efficiency of GaN-based devices. The two main obstacles faced in the quest for Ohmic contacts of low specific contact resistivity to p-GaN were recognized to be the difficulty in growing a heavily doped p-GaN (more than 10^{18} cm^{-3}) and the absence of appropriate metals having work function larger than that of p-GaN (~7.5 eV). These problems have led to several attempts in finding Ohmic contacts with low specific contact resistance

to p-GaN (Lim woon chi, 2006). Therefore, the investigation of Au-free (Ni/Cu) Ohmic contact on p-type GaN heterostructures to solve surface roughness issues are the topic that worth to research.

2.3 Metal System with their Low Specific Contact Resistivity

The instability of metal to semiconductor contacts at higher temperatures arises due to factors such as thermodynamic instability at the interface, lack of chemical inertness especially to oxygen containing ambient and a large lattice mismatch to the substrate (Lee et al., 1998).

The most widely used Ohmic contact for AlGaN/GaN HEMT devices is the alloy of a multilayer metal structure that consists of Ti/Al metal layers. These layers will form a low resistance alloy upon annealing at high temperature (750–950°C) and the mechanism is well documented. Since Ti/Al is prone to oxidation, an oxidation prevention layer such as gold (Au) is deposited on Ti/Al to protect the Ohmic contact for long term device operation. Finally, a barrier layer (such as Ni, Cr, Pt, or Mo) is also needed to prevent Au from diffusing into GaN during thermal annealing process. By optimizing the Ohmic contact formation parameters, specific contact resistances (ρ_c) as low as 7.3 x 10^{-7} Ωcm^2 (Wenzel et al., 2001) and 4.7 x 10^{-7} Ωcm^2 (Guo et al., 1996) have been demonstrated using Ti/Al/Ni/Au and Ti/Al/Mo/Au Ohmic structure, respectively.

However, the ever rising gold cost on a long-term basis has fueled the search for an alternative material to replace the Au layer for GaN device metallization. In this context, the

copper (Cu) is a potential candidate. Besides the cost issue, Cu also has lower resistivity and higher thermal conductivity as compared with Au. Therefore, the Cu has been widely used for multi-level interconnects in the silicon VLSI technology (Schmitz et al., 1998, Adivarahan et al., 2001).

These advantages will certainly generate much interest in using Cu metallization on GaN devices as well. In fact, Cu has been demonstrated to perform well as gate contacts (Shen et al., 1992) and as interconnects (Nakamura et al., 1993) on the GaN HEMTs. Nevertheless, the diffusion of Cu into GaN at elevated temperatures can be detrimental to the GaN devices (Chen et al., 1999).

An effective diffusion barrier to Cu is thus required, especially for the Ohmic contact. A few Ohmic contact structures for GaN devices, such as Si/Ti/Al/Cu/Au (Koide et al., 1999) and Ge/Cu/Ge (Waki et al., 2000) have been investigated. Although Ohmic contacts could be achieved at relatively lower temperatures (<800°C) for these structures, they all suffer from having high contact resistance ($\rho_c > 10^{-5}$ Ωcm^2). In this study, the feasibility of using Ti/Al/Ni/Cu were investigate as the Ohmic contact material for AlGaN/GaN structures. This metal stack differs from the conventional Ti/Al/Ni/Au in that the top metal Au is replaced by Cu. The Ti/Al layers were adopted to achieve good Ohmic contact. The role of Ni as an adhesion and diffusion barrier layer will also be examined. They show that, with an optimized Ni layer thickness, a low contact resistance and smooth surface morphology can be achieved with the Ti/Al/Ni/Cu Ohmic contact (Waki et al., 2000).

Ti/Al/Ni/Cu Ohmic contact for AlGaN/GaN structure has been fabricated. The Ni layer played an important role in achieving low specific contact resistance (ρ_c), smooth

morphology, and excellent edge acuity. With a 50 Å Ni layer, a ρ_c of 1.35 x 10^{-6} Ωcm^2 and a root-mean-square roughness of 7.65 nm have been realized. The characterization results indicated that no evidence of Cu diffusion into the semiconductor layers. The formation of Al-Cu and Ti-Cu alloys might have confined the Cu within the Ohmic metal. In the absence of gold, the surface roughening caused by Au-Al alloy in conventional Ti/Al/Ni/Au structure was also prevented (Wong et al., 2013).

The specific contact resistances, ρ_c, of metal systems on p-GaN tabulated in Table 2.1. It is tabulated in increasing order of ρ_c and indicates the conditions under which the ρ_c was obtained: thickness of metal layers used, doping concentration of GaN and annealing conditions.

Table 2.1: Metal contacts with the lowest specific contact resistances (ρ_c), the thickness of metal layers, doping concentration of GaN and annealing conditions are indicated. Contacts are arranged in ascending order of ρ_c.

No.	Reference	Metal Contacts	Specific contact resistance, ρ_c (Ω cm^2)	Metal Thickness (nm)	Annealing Conditions: Temp/Ambient /Time	Doping conc. of p-GaN (cm^{-3})
1	(Jacobs et al., 2002)	Ti/Al/Ni/Au	7.3×10^{-7}	30/180/40/150	900 °C (N_2) 30s	
2	(Kumar et al., 2002)	Ti/Al/Mo/Au	4.7×10^{-7}	15/60/35/50	850 °C (N_2) 30s	
3	(Adivarahan et al., 2001)	Pd/Ag/Au/Ti/Au	1.0×10^{-6}		800°C (N_2)	
4	(Wong et al., 2013)	Ti/Al/Ni/Cu	1.35×10^{-6}	20/120/25/100	900 °C (N_2) 30s	

5	(Lim woon chi, 2006)	Pt/Ru	2.2×10^{-6}	20/50	600 °C (N_2) 2min	$2\text{-}3\times10^{17}$
6	(Lim woon chi, 2006)	Ni/Au	4×10^{-6}	5/5	500 °C (O_2) 10min	2×10^{17}
7	(Lim woon chi, 2006)	Ni/AZO	6.23×10^{-6}	5/450	550 °C (air) 5min	5×10^{17}
8	(Lim woon chi, 2006)	Rh/Au	9.3×10^{-6}	5/5	As-deposited (i.e., no annealing)	4×10^{17}
5	(Lim woon chi, 2006)	Rh	1.7×10^{-5}	10	As-deposited (i.e., no annealing)	4×10^{17}
6	(Lim woon chi, 2006)	Au/Ni/Au	$\sim 10^{-5}$	5/8/4	500 °C (air) 10min	$2\text{-}5\times10^{17}$
7	(Lim woon chi, 2006)	Ir/Ni	3.4×10^{-5}	5/5	500 °C (O_2) 1min	3×10^{17}
8	(Suzuki et al., 1999)	Ta/Ti	3.0×10^{-5}		800°C, vacuum, time not specified	
9	(Jang et al., 2002)	Ru/Ni	4.5×10^{-5}		500°C (O_2) time not specified	
10	(Lim woon chi, 2006)	Ti/Pt/Au	4.2×10^{-5}	15/50/80	800 °C (N_2) 2min	2.5×10^{17}
11	(Lim woon chi, 2006)	Ru/Ni	4.5×10^{-5}	5/5	500 °C (O_2) 1min	3×10^{17}
12	(Lim woon chi, 2006)	Pd/Ni	5.7×10^{-5}	3/7	500 °C (O_2) 1min	3.3×10^{17}
13	(Lim woon chi, 2006)	Rh/Ni	6×10^{-5}	5/5	As-deposited	4×10^{17}
14	(Mahadik et al., 2005)	Cu/Ge/Ti	9.1×10^{-5}	40/70/25	690°C (Ar) 10 min	9.2×10^{17}
15	(Lim woon chi, 2006)	Ni/Pd/Au	1×10^{-4}	20/20/100	500 °C (O_2) 5min	4.1×10^{17}

16	(Lim woon chi, 2006)	Ni/Au	1×10^{-4}	10/5	500 °C (N_2) 10min	2×10^{17}
17	(Lim woon chi, 2006)	Ni/Pd/Au	1.0×10^{-4}		550°C (O_2)	
18	(Liu et al., 2003)	Ni/Cu	1.31×10^{-4}	20/20	600°C (N_2) 30s	3.0×10^{17}
19	(Wenzel et al., 2001)	Cr/Au	3.0×10^{-4}		500 °C (N_2) 1 min	1.4×10^{20}
20	(Crofton, 1992)	Pd/Ni/Au	5.03×10^{-4}	20/30/200	450 °C (N_2) 2min	1.0×10^{18}
21	(Jang et al., 1999)	Pt/Ni/Au	5.1×10^{-4}	20/30/80	350 °C (N_2) 1min	3×10^{17}
22	(Lim woon chi, 2006)	Ni/ITO	8.6×10^{-4}	10/250	600 °C (air) 2min	$\sim2\times10^{17}$
23	(Lim woon chi, 2006)	Ni/Au	Low-10^{-3}	10/40	500 °C (O_2/N_2) 5-15min	6-7×10^{17}
24	(Reddy et al., 2004)	Pt/Re/Au	1.4×10^{-3}	20/30/80	600°C (N_2) 1 min	1.13×10^{17}
25	(Wenzel et al., 2001)	Pt/Au	1.5×10^{-3}		750 °C, 10min	6.0×10^{16}
26	(Gaskill et al., 1996)	Pt/Au	2.0×10^{-3}		Temperature not specified, 1min	1.4×10^{20}
27	(Wenzel et al., 2001).	Ni/Zn-Au	3.6×10^{-3}	Unknown	600 °C, 2min	4.4×10^{17}
28	(Wenzel et al., 2001)	Pt/Au	2.0-8.0×10^{-3}	50/200	700 °C (before metallization) 15min 750 °C (after)	Unknown
29	(Chu et al., 2000)	Pd/Au	9.1×10^{-3}		500 °C, 30s	9.1×10^{16}
30	(Lim woon chi, 2006)	Pt/Au	High-10^{-3}	10/40	300-600 °C (O_2/N_2)	6-7×10^{17}

31	(Lim woon chi, 2006)	Pt	High-10^{-3}	50	600 °C (O_2/N_2) 5min	6-7×10^{17}
32	(Zhou et al., 2000)	Ni/Au	10^{-2}		500 °C, time not specified	10^{17}-10^{18}
33	(Jang et al., 2002)	Ni/Si	1.0×10^{-2}		400 °C, 30min	3.0×10^{17}
34	(Jang et al., 1998)	Ni/Pt/Au	2.1×10^{-2}		500°C (Ar)	
35	(Jang et al., 2001)	Ni/Cr/Au	8.3×10^{-2}		500 °C, 30s	1.0×10^{17}
36	(Chuah et al., 2010)	Ni/Ag	1.74×10^{-1}	300/100	700°C (N_2) 15 min	4×10^{20}
37	(Chen et al., 1999)	Cr/Au	4.3×10^{-1}		900 °C, 15s	9.8×10^{16}
38	(Hassan et al., 2004)	Ni/Ag	3.5×10^{-1}		800°C (N_2)	

From the literature, few researchers used metal copper (Cu) as metal contact to n-GaN, and it is rarely used as metal contacts to p-GaN, commercially used as an Ohmic contact to p-type GaN. This specific metallization scheme was deemed to be stable and it has been reported in the literature that Ni/Au based bi-layer structures are capable of forming Ohmic contacts to p-GaN providing a specific contact resistivity in the range of 10^{-2} to 10^{-6} Ωcm^2. Nickel was selected as the metal at the interface between metal and semiconductor due to its ability to diffuse through the oxide contamination layer between the Cu and GaN and reach directly in contact with GaN itself. The selection of Cu as capping layer was motivated by the thermal stability of the metals, the melting point for Cu is 1085 °C. Therefore, samples with fabricated Ni/Cu on p-type GaN which were nickel based metallization were able to be annealed until 800 °C to investigate the electrical properties as well as the thermal stability of the samples (Chuah et al., 2010).

2.4 Cu-Ni Alloys

2.4.1 General Information on Cu-Ni Alloys

In 1751, A.F. Cronstedt succeeded in isolating nickel. However, Cu-Ni alloys were in existence much earlier, mostly prepared by processing ores. Today, Cu-Ni alloys have gained a variety of interesting applications because of their specific characteristics. Copper and nickel are adjacent to one another in the periodic system of elements, with atomic numbers 29 and 28 and atomic weights 63.54 and 68.71.The two elements are closely related and are completely miscible in both the liquid and solid state. Cu-Ni alloys crystallize over the whole concentration range in a face-centred cubic lattice. The lattice spacing of the face-centre cubic solid solution varies almost linearly with atomic concentration between the values for copper (3.1653×10^{-8} cm) and that for nickel (3.5238×10^{-8} cm) (Kupferinstitut, 1965).

2.4.2 The Cu-Ni equilibrium diagram

The equilibrium diagram was first established by Gürtler and Tammann and was later improved by Pilling and Kihlgren, among others. Figure 2.2 shows the Cu-Ni equilibrium diagram. Alloys of the two metals form a continuous series of solid solutions having a face-centred cubic lattice, i.e. the Cu-Ni system exhibits complete solubility in both liquid and solid states. The equilibrium diagram is therefore very simple. The melting points of the two components broaden to a melting range in the alloys. The upper curve, which forms the lower boundary of the liquid melt, is called the ‘liquidus’. The curve which forms the upper

boundary of the area of a crystals is termed the ‘solidus’. A two-phase area in which liquid and a crystals co-exist is formed between liquidus and solidus (Brown and William, 1968).

Below a dotted straight line at the bottom right, behaviour is ferromagnetic, above it is paramagnetic. Thus, for example all alloys up to 80% Ni are paramagnetic at 150 ºC while at 20 ºC alloys containing more than 68.5% nickel exhibit ferromagnetic behavior (Brown and William, 1968).

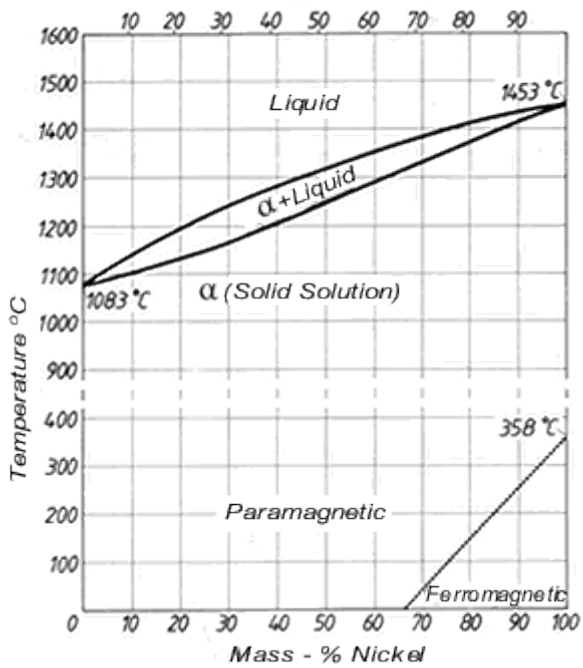

Figure 2.1 : Cu-Ni equilibrium diagram (Brown and William, 1968).

2.5 Circular Transmission Line Model (CTLM)

2.5.1 Basic Concept of CTLM

The Circular Linear Transmission Line Model (CTLM) is a widely-used model for measuring specific contact resistance, ρ_c, which is the resistance at the interface between the metal and the semiconductor. The CTLM structure is basically the same as the linear-TLM in terms of measurement and contact parameter extraction, but with a different layout. The CTLM structure consist of circular metal contacts with ring shaped as spacing d between the inner circle and outer (Reeves, 1980). The contact geometry is shown in Figure 2.3.

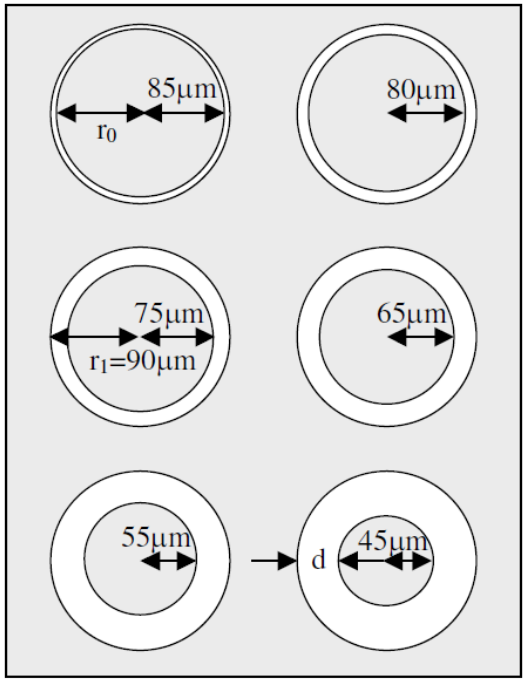

Figure 2.2: Test pattern for Ohmic contact characterization: Circular pattern, where r_o is the radii of the inner circular contact; r_i is the radii of the outer region; and d is the difference between r_o and r_i (Schroder, 2006).

2.5.2 Derivation of Specific Contact Resistance

By having a constant current (i_o) through the inner circular and outer contact pads using a Precision Parameter Analyzer, as indicated in Figure 2.3, there will be a voltage drop, ΔV, across the separation (d) between two points.

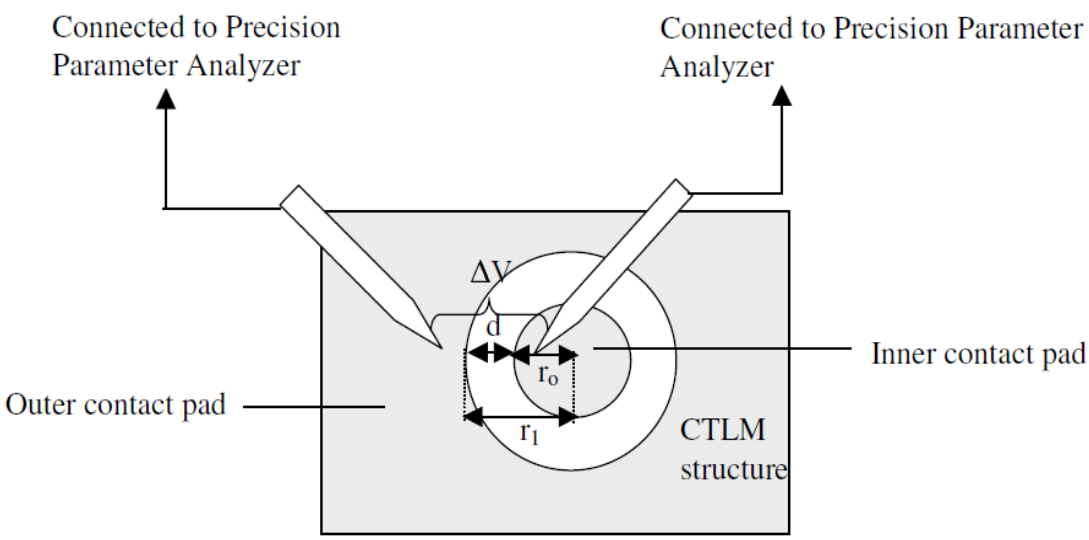

Figure 2.3: Experimental setup for deviation of specific contact resistance (Schroder, 2006).

The voltage drop across the separation *d*, is given by:

$$\Delta V = \frac{i_o R_s}{2\pi}\left[\ln\left(\frac{r_1}{r_o}\right) + \frac{L_T}{r_o}\frac{I_o(r_o/L_T)}{I_1(r_o/L_T)} + \frac{L_T K_o}{r_1 K_1}\frac{(r_1/L_T)}{(r_1/L_T)}\right] \tag{2.1}$$

where i_o = Current across the separation, d;

R_s = Semiconductor sheet resistance;

L_T = Transfer length;

I_o, I_1, K_o, K_1 = Modified Bessel Functions; and

r_o , r_1 = Radii of the inner circular contact and the outer region that define the separation d (referring to Figure 2.3).

The transfer length, L_T, is related to the specific contact resistance, ρ_c, of the metal/semiconductor contact and the sheet resistance, R_s, of the semiconductor, and is given by:

$$L_T = \sqrt{\left(\frac{\rho_c}{R_s}\right)} \tag{2.2}$$

In cases where r_i and r_o are greater than L_T by a factor of at least 4, both I_o/I_1 and K_o/K_1 approximate to unity (Adivarahan et al., 2001). Thus, Equation 2.1 become:

$$\Delta V = \frac{iR_S}{2\pi}\left[\ln\left(\frac{r_o}{r_o - d}\right) + L_T\left(\frac{1}{r_o} + \frac{1}{r_o - d}\right)\right] \tag{2.3}$$

The total resistance, R_T, between the contacts is defined as the ratio of the voltage across the separation (ΔV) and the current (i), i.e. $R_T = \Delta V / i$, hence,

$$R_T = \frac{R_S}{2\pi}\left[\ln\left(\frac{r_o}{r_o - d}\right) + L_T\left(\frac{1}{r_o} + \frac{1}{r_o - d}\right)\right] \tag{2.4}$$

And since $2\pi(r_o - d) \gg d$, Equation 2.1 can be simplified to

$$R_T = \frac{R_S}{2\pi r_o}\left[d + 2L_T\right] \tag{2.5}$$

where R_T includes the probe resistance. However, the probe resistance is normally very small and hence it can be ignored.

From Equation 2.5, a linear relationship were shown between R_T and the circular contact pad spacing, d. Hence, a graph of R_T versus d can be plotted, as shown in Figure 2.4, in order to determine the value of ρ_c.

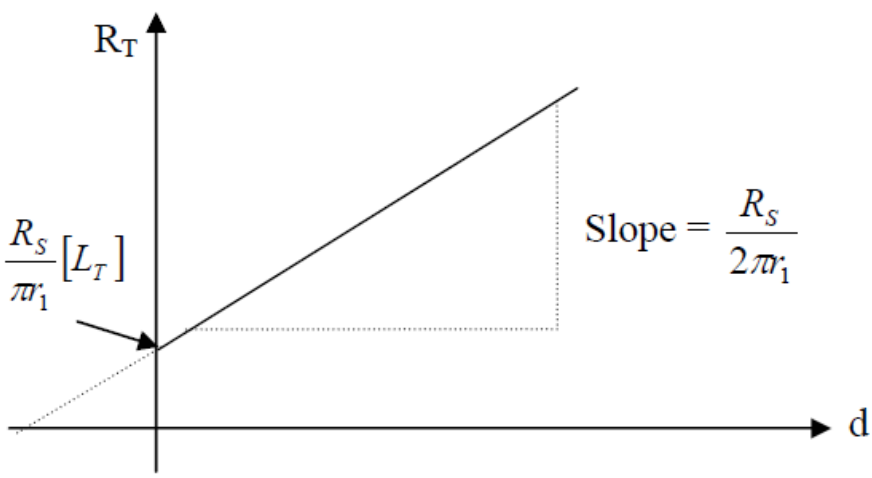

Figure 2.4: Graph of R_T versus d used to calculate specific contact resistance ρ_c of metal contact (Schroder, 2006).

The slope of the graph shown in Figure 2.4 gives the value of $R_s/2\pi r_o$ and the interception with the vertical R_T-axis gives the value of $R_s (L_T) / \pi r_1$. Hence, the value of the transfer length, L_T, can be obtained by dividing the y-interception over the slope:

$$L_T = (\text{y-interception} / \text{slope}) \times 2 \tag{2.6}$$

From Equation 2.2, the value of specific contact resistance, ρ_c, can then be obtained:

$$\rho_{c,} = (L_T)^2 \times R_s \tag{2.7}$$

The transmission line model (TLM) and the circular transmission line model (CTLM) are the two most commonly applied methods to extract the contact resistivity, ρ_c, from the contact resistance, ρ_c. For higher values of ρ_c, the metal resistance impact is negligible. However, when ρ_c becomes lower, neglecting the metal resistance can easily lead to a misinterpretation of ρ_c and an inaccurate extraction of ρ_c. Linear TLM technique tends to suffer from the fact that currents from one contact to another contact may spread due to current crowding. The main limitation of TLM structure is that it is a differential measurement and the sheet resistance is measured along with the contact resistance This limits the accuracy of data extraction to the errors in determining the geometrical values of depth, width and length of the pattern developed (Roy, 2011).

Compared with TLM, CTLM benefits from its easier process and especially suits the quick contact scheme screening. The main advantage of the CTLM is that it is not necessary to isolate the diffused or implanted layer like for the Linear Transmission Line Model (CTLM) where current can flow from contact to contact through the region beyond the structure in the linear arrangement (if it is not isolated). In the circular case, current can only flow from the center to the surrounding contact and no other path is possible. Besides that, CTLM is easier to realize using simple process steps. It enables the use of a wide range of metals, since no patterning steps are required after metal deposition. Unlike the traditional linear TLM, the CTLM has the advantage of not requiring etch. Using a lift-off resist process realization therefore just takes one lithography step. It also enables the investigation of the influence of different anneal steps on the contact resistance without destroying the transistor, or using expensive full grown active device substrates (Klootwijk and Timmering, 2004).

2.6 Physics of metal-semiconductor contact

2.6.1 Schottky-Mott Model

According to the Schottky-Mott model, a Schottky barrier is formed when a metal comes into contact with a semiconductor, which is due to the difference in the work functions of the metal and the semiconductor. This is illustrated in the energy band diagrams shown in Figure 2.5 for p-type (Sze, 1981).

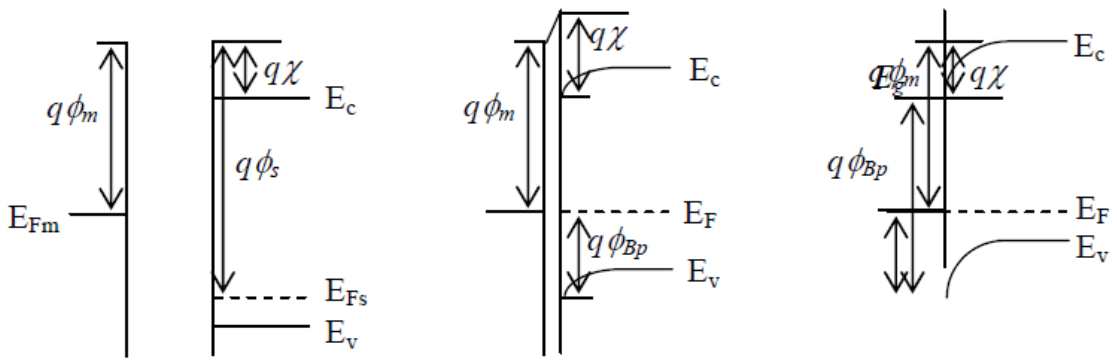

(a) p-type $q\varphi_m < q\varphi_s$ (rectifying).

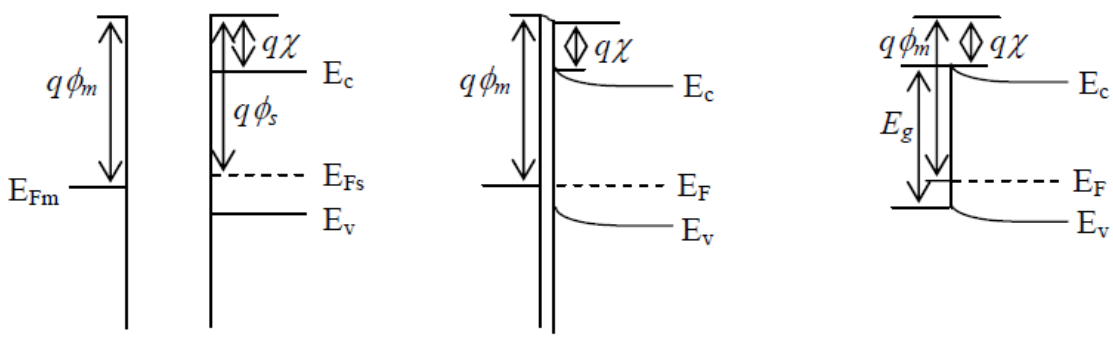

(b) p-type $q\varphi_m > q\varphi_s$ (ohmic).

Figure 2.5: Energy band diagrams of metal-semiconductor contacts (Sze, 1981).

The height of the Schottky barrier for p-type semiconductor ($q\varphi_{Bp}$) measured with respect to the Fermi level is given by (Sze, 1981):